
Journal Articles: Oncology and Hematology

Oncology and Hematology

Winter 1-1-2015

Targeted mutational profiling of peripheral T-cell lymphoma not otherwise specified highlights new mechanisms in a heterogeneous pathogenesis.

J. H. Schatz
University of Arizona

S. M. Horwitz
New York University Langone Medical Center

J. Teruya-Feldstein
New York University Langone Medical Center

Matthew A. Lunning
University of Nebraska Medical Center, mlunning@unmc.edu

A. Viale
New York University Langone Medical Center

Tell us how you used this information in this [short survey](#).

Follow this and additional works at: https://digitalcommons.unmc.edu/com_onchem_articles
See next page for additional authors

 Part of the [Hematology Commons](#), and the [Oncology Commons](#)

Recommended Citation

Schatz, J. H.; Horwitz, S. M.; Teruya-Feldstein, J.; Lunning, Matthew A.; Viale, A.; Huberman, K.; Soccia, N. D.; Lailler, N.; Heguy, A.; Dolgalev, I.; Migliacci, J. C.; Pirun, M.; Palomba, M. L.; Weinstock, D. M.; and Wendel, H-G, "Targeted mutational profiling of peripheral T-cell lymphoma not otherwise specified highlights new mechanisms in a heterogeneous pathogenesis." (2015). *Journal Articles: Oncology and Hematology*. 4.
https://digitalcommons.unmc.edu/com_onchem_articles/4

This Article is brought to you for free and open access by the Oncology and Hematology at DigitalCommons@UNMC. It has been accepted for inclusion in Journal Articles: Oncology and Hematology by an authorized administrator of DigitalCommons@UNMC. For more information, please contact digitalcommons@unmc.edu.

Authors

J. H. Schatz, S. M. Horwitz, J. Teruya-Feldstein, Matthew A. Lunning, A. Viale, K. Huberman, N. D. Socci, N. Lailler, A. Heguy, I. Dolgalev, J. C. Migliacci, M. Pirun, M. L. Palomba, D. M. Weinstock, and H-G Wendel

oncostatin M.¹³ Considering that lack of paracrine IL-6 prolonged PCT onset by ~50%, it is likely that targeting IL-6 production in human bone marrow stromal cells would slow the transition from MGUS¹⁴ to frank MM with similar efficiency, potentially preventing many cases of newly diagnosed disease. The adoptive cell transfer approach described here can be readily extended to studies on other myeloma drivers that govern complex tumor-TME interactions, such as Bruton tyrosine kinase (BTK).¹⁵ For example, complementary transfers of Myc⁺BTK⁻ B cells to BTK⁺ hosts or Myc⁺BTK⁺ B cells to BTK⁻ hosts may further our understanding of the specific function of BTK in myeloma cells vs osteoclasts and, thereby, provide preclinical support for the clinical testing of small-compound BTK inhibitors in myeloma.

CONFLICT OF INTEREST

The authors declare no conflict of interest.

ACKNOWLEDGEMENTS

This research was performed by TRR in partial fulfillment of the requirements for the degree Doctor of Philosophy in the Graduate Immunology Program of the University of Iowa. We thank Kristin Ness for expert mouse husbandry. This work was supported in part by NIH Predoctoral Training Grant 5T32 AI007485 (TRR), by the Intramural Research Program of the NIAID (to HCM), by NCI Core Grant P30CA086862 in support of The University of Iowa Holden Comprehensive Cancer Center, by a Senior Research Award from the Multiple Myeloma Research Foundation (to SJ), by a research award from the International Waldenström's Macroglobulinemia Foundation (to SJ), by a NCI P50CA097274 career development award (to SJ), and by R01CA151354 from the NCI (to SJ).

TR Rosean¹, VS Tompkins², AK Olivier², R Sompallae^{2,3}, LA Norian^{1,4}, HC Morse III⁵, TJ Waldschmidt^{1,2} and S Janz^{1,2}

¹Interdisciplinary Graduate Program in Immunology, University of Iowa (UI), Iowa City, IA, USA;

²Department of Pathology, UI Carver College of Medicine, Iowa City, IA, USA;

³Bioinformatics Core Facility, UI Carver College of Medicine, Iowa City, IA, USA;

⁴Department of Urology, UI Carver College of Medicine, Iowa City, IA, USA and

⁵Laboratory of Immunogenetics, NIAID, NIH, Rockville, MD, USA

E-mail: siegfried-janz@uiowa.edu

Supplementary Information accompanies this paper on the Leukemia website (<http://www.nature.com/leu>)

OPEN

Targeted mutational profiling of peripheral T-cell lymphoma not otherwise specified highlights new mechanisms in a heterogeneous pathogenesis

Leukemia (2015) 29, 237–241; doi:10.1038/leu.2014.261

Peripheral T-cell lymphoma not otherwise specified (PTCL-NOS) is a diagnosis of exclusion making up the largest fraction (25–30%) of PTCL. Although traditionally considered a 'wastebasket' diagnosis, recent gene-expression results suggest the disease comprises two biologic sub-entities characterized by expression of

Letters to the Editor

REFERENCES

- Anderson KC, Carrasco RD. Pathogenesis of myeloma. *Annual Rev Pathol* 2011; **6**: 249–274.
- Rajkumar SV. Preventive strategies in monoclonal gammopathy of undetermined significance and smoldering multiple myeloma. *Am J Hematol* 2012; **87**: 453–454.
- Kawano M, Hirano T, Matsuda T, Taga T, Horii Y, Iwato K et al. Autocrine generation and requirement of BSF-2/IL-6 for human multiple myelomas. *Nature* 1988; **332**: 83–85.
- Klein B, Zhang XG, Jourdan M, Content J, Houssiau F, Aarden L et al. Paracrine rather than autocrine regulation of myeloma-cell growth and differentiation by interleukin-6. *Blood* 1989; **73**: 517–526.
- Fulciniti M, Hidemitsu T, Vermot-Deroches C, Pozzi S, Nanjappa P, Shen Z et al. A high-affinity fully human anti-IL-6 mAb, 1339, for the treatment of multiple myeloma. *Clin Cancer Res* 2009; **15**: 7144–7152.
- Chari A, Pri-Chen H, Jagannath S. Complete remission achieved with single agent CNTO 328, an anti-IL-6 monoclonal antibody, in relapsed and refractory myeloma. *Clin Lymphoma Myeloma Leuk* 2013; **13**: 333–337.
- Duncan K, Rosean TR, Tompkins VS, Olivier A, Sompallae R, Zhan F et al. (18)F-FDG-PET/CT imaging in an IL-6- and MYC-driven mouse model of human multiple myeloma affords objective evaluation of plasma cell tumor progression and therapeutic response to the proteasome inhibitor ixazomib. *Blood Cancer J* 2013; **3**: e165.
- Park SS, Shaffer AL, Kim JS, duBois W, Potter M, Staudt LM et al. Insertion of Myc into IgH accelerates peritoneal plasmacytomas in mice. *Cancer Res* 2005; **65**: 7644–7652.
- Lattanzio G, Liberi C, Aquilina M, Cappelletti M, Ciliberto G, Musiani P et al. Defective development of pristane-oil-induced plasmacytomas in interleukin-6-deficient BALB/c mice. *Am J Pathol* 1997; **151**: 689–696.
- Shacter E, Arzadon GK, Williams J. Elevation of interleukin-6 in response to a chronic inflammatory stimulus in mice: inhibition by indomethacin. *Blood* 1992; **80**: 194–202.
- Hilbert DM, Migone TS, Kopf M, Leonard WJ, Rudikoff S. Distinct tumorigenic potential of abl and raf in B cell neoplasia: abl activates the IL-6 signaling pathway. *Immunity* 1996; **5**: 81–89.
- Hodge LS, Ziesmer SC, Yang ZZ, Secreto FJ, Gertz MA, Novak AJ et al. IL-21 in the bone marrow microenvironment contributes to IgM secretion and proliferation of malignant cells in Waldenstrom macroglobulinemia. *Blood* 2012; **120**: 3774–3782.
- Taniguchi K, Karin M. IL-6 and related cytokines as the critical lynchpins between inflammation and cancer. *Semin Immunol* 2014; **26**: 54–74.
- Weiss BM, Abadie J, Verma P, Howard RS, Kuehl WM. A monoclonal gammopathy precedes multiple myeloma in most patients. *Blood* 2009; **113**: 5418–5422.
- Tai YT, Chang BY, Kong SY, Fulciniti M, Yang G, Calle Y et al. Bruton tyrosine kinase inhibition is a novel therapeutic strategy targeting tumor in the bone marrow microenvironment in multiple myeloma. *Blood* 2012; **120**: 1877–1887.

Accepted article preview online 3 September 2014; advance online publication, 26 September 2014

the transcription factors GATA3 or TBX21 and their target genes.¹ The mutational landscape of PTCL-NOS remains largely undefined.

We sought a better understanding the disease using a targeted deep-sequencing approach to identify pathogenic mechanisms and potential therapeutic targets that might fuel further studies. There is a substantial need for new therapies for PTCL-NOS, which leads to the death of more than two-thirds of patients within 5 years of diagnosis.² The median age of onset for PTCL-NOS is 60,

two-thirds of patients are male, and 69% have advanced-stage at diagnosis. Front line treatment remains CHOP (cyclophosphamide, doxorubicin, vincristine and prednisone) or other CHOP-based combinations optimized for use in B-cell lymphomas. Efforts to address the substantial unmet clinical need of PTCL-NOS patients are hampered by poor understanding of its biology, thwarting the development of specific therapies.

We collected 61 formalin-fixed paraffin embedded (FFPE) tumor samples from patients seen at Memorial Sloan-Kettering Cancer Center (MSKCC) with original diagnosis of PTCL-NOS, anaplastic large-cell lymphoma (ALCL) or angioimmunoblastic T-cell lymphoma (AITL). After re-review (JTF) of pathology and clinical factors, 31 cases met criteria for inclusion in this study of PTCL-NOS, lacking features indicative of other PTCL types. Pathologic details including morphology and immunophenotype are provided in Supplementary Table 1. In particular, we excluded cases with features of AITL because several studies have illuminated its mutational landscape,^{3–7} while our interest was in PTCL-NOS, for which few disease-specific recurrent mutational targets have been reported. We chose 237 genes for deep sequencing that have been reported as recurrent mutational targets in other hematologic cancers (Supplementary Table 2).

Analyzed tumor samples came from patients who consented to institutional tissue banking and analysis protocols, approved by the MSKCC Institutional Review Board and in compliance with the Declaration of Helsinki. Specific authorization for use and collection of de-identified clinical data came from the Human Biospecimen Use Committee. We isolated DNA from FFPE scrolls using the Formapure kit from Beckman Coulter Genomics in a semi-automated fashion on a Biomek NX liquid Handler. Illumina-compatible libraries were prepared from ~250 ng of sheared DNA (~150 bp in size) on a Biomek SPRI-Works HT robot using the Kapa Biosystems High Throughput library preparation kit with SPRI solution (magnetic beads) and amplified using the Kapa Standard PCR Library Amplification/Illumina series. During library preparation, adapters with barcodes were added to the DNA fragments for sample identification. All exons of the 237 genes were captured using the Nimblegen system (Roche SeqCap EZ Custom bait hybridization probes). The samples were then pooled and run on an Illumina HiSeq sequencer.

Reads were aligned to the hg19 build of the human genome using BWA 0.6.2-r126 followed by duplicate removal using Picard-Tools-1.55. The Genome Analysis Toolkit (GATK-2.6-3-gdee51c4) was used to perform local realignment around known indels and base quality score recalibration. Variant detection was performed using the GATK Unified Genotyper. Quality settings in the GATK HaplotypeCaller resulted in the elimination of candidate variants at very low allele frequency, which while improving the overall confidence of reported mutations likely also excluded some tumor-specific sub-clonal variants. Variants were annotated with the SNPeff annotation program to identify protein-coding changes and cross-referenced against the dbSNP132, 1000 Genomes and Catalog of Somatic Mutations in Cancer (COSMIC) databases. We eliminated variants listed in dbSNP132 or 1000 genomes and reviewed all remaining variants manually in IGV 2.3 browser, resulting in the elimination of additional mutation calls based on sequencing quality, allele frequency (if similar to known single-nucleotide polymorphisms (SNPs) in the same sample) and by searching the internet to identify additional SNPs. Mean sequencing depth was 232X (range 6–701). Cases with mean sequencing depth <100X (7 of 31) were included only if mutations were confirmed by targeting validation sequencing (see below), resulting in inclusion of four and exclusion of three such cases. This left 28 total cases for which we report mutations. Targeted validation sequencing of all mutations was performed with Illumina miSeq after re-amplification of DNA from the FFPE tumor samples, again using the Nimblegen capture system.

Of 28 patients, 25 with available demographic data were an average age of 52 years at diagnosis (range 9–76), with 11/25 age ≥60 and 13/25 male. Treatment and survival data were available for 23 patients followed long term at MSKCC. The majority of these (16) received CHOP or CHOP-like chemotherapy (Supplementary Figure 1A), whereas three received more intensive chemotherapy. Median event-free survival was 11.5 months, whereas median overall survival (OS) was 40.2 months (Supplementary Figure 1B). Subjects showed somewhat lower average age and less male predominance than is typical.² There was no OS difference between cases with nodal or extranodal presentation (Supplementary Figure 1C). Twenty-four of 28 samples were pretreatment and 4 were relapsed.

Table 1 shows 89 protein-coding mutations found in the 28 cases, affecting 59 genes, including 74 single-nucleotide variants and 15 indels. There was a mean of 3.0 mutations per case (range 0–11). There was no significant difference between the mutational load in the four relapsed samples and others ($P=0.283$), but we can't exclude the possibility some mutations detected in these four samples were not present at diagnosis. Lack of germ-line DNA to confirm the somatic nature of mutations introduces the possibility that some mutations in Table 1 are SNPs that are not reported in dbSNP132 or detected in the 1000 genomes project. We therefore limited further analysis to genes either recurrently mutated or containing mutations previously shown to be tumor specific in other studies. Figure 1 shows breakdown of genes affected by such mutations by functional category and whether cases had a nodal or extranodal presentation.

As seen in other hematologic cancers, epigenetic regulation is the most mutated category overall. Regulators of histone methylation were mutated in 25% of cases, including *MLL2*⁸ (4/28 cases), *KDM6A* (3/28) and *MLL* (2/28). Regulators of DNA methylation also were affected in 25% of cases. *TET2* showed previously reported frameshifts in two cases and a missense mutation in a third, whereas *DNMT3A* had a frameshift in one case and a previously reported missense mutation in a second. The significance of two previously unreported *TET1* missense mutations is less clear. There was no overlap between cases with histone methylation and DNA methylation alterations (Supplementary Figure 2A). Chromatin remodeling mediated by SWI/SNF complex activity is affected in 18%, specifically, *ARID1B* (3/28 cases), *ARID2* (1/28) and *SMARCA2* (1/28). These frequencies are similar to a recent meta-analysis of 44 cancer-sequencing studies.⁹ Overall, epigenetic regulators emerge as recurrent targets of somatic mutations in PTCL-NOS.

Activation of T-cell receptor (TCR) signaling is a known pathogenic mechanism in PTCL-NOS containing t(5;9)(q33;q22), found in <10 percent of cases.¹⁰ The resulting ITK-SYK fusion kinase localizes to lipid-rafts and mimics constitutive TCR activation.¹¹ Our data highlight additional mechanisms activating TCR and downstream signaling. *TNFAIP3*, encoding the A20-negative regulator of NF- κ B activation, had missense mutations in 11% (3/28) of cases, all of which are reported in the COSMIC. A20 is known to be a key regulator of NF- κ B activation in T cells after TCR stimulation.¹² WNT/ β -Catenin negative regulators *APC* and *CHD8* were affected in two cases each, or 14% (4/28) overall. Three additional genes with known suppressive roles in TCR activation had mutations previously reported in COSMIC: *NF1* (frameshift), *TNFRSF14* (missense affecting the start codon) and *TRAF3* (nonsense). Overall, 46% (13/28) had at least one mutation in TCR or downstream mediators, expanding the role for these processes in PTCL-NOS pathogenesis.

The *TP53* tumor suppressor gene had loss-of-function alterations in two cases, consistent with prior reports showing it is not mutated at a high rate in PTCL.^{13,14} Additional affected suppressors include the *ATM* DNA-repair kinase (one case) and the transcription factors *FOXO1* and *BCORL1* (two cases each).

Table 1. Protein-affecting variants by gene and case

Gene	Case	CHR	POS	REF	ALT	Mutant Allele Fraction	Type	Effect	Previous Report
ALMS1	T06	chr2	73 676 742	T	A	0.39444	Missense	p.S1029T	None
ALPK2	T46	chr18	56 203 629	C	T	0.35000	Missense	p.G1264S	None
APC	99-31720	chr5	112 164 629	G	A	0.50131	Missense	p.S568N	COSMIC
APC	T52	chr5	112 176 308	G	A	0.42678	Missense	p.E1673K	COSMIC
ARID1B	T11	chr6	157 099 420	G	GCAGCAA	0.33333	Codon insertion	p.119_120insQQ	None
ARID1B	T33	chr6	157 431 662	G	A	0.42798	Missense	p.A709T	None
ARID1B	T56	chr6	157 528 066	CTG	C	0.44118	Frameshift	p.C1932fs	None
ARID2	99-31720	chr12	46 125 011	GA	G	0.28737	Frameshift	p.N67fs	COSMIC
ATM	T37	chr11	108 160 480	T	G	0.44118	Missense	p.F1463C	COSMIC
BCL6	T34	chr3	187 447 027	T	C	0.41648	Missense	p.N389S	None
BCL9	T55	chr1	147 095 762	C	T	0.41615	Missense	p.P1095S	None
BCORL1	T11	chrX	129 150 080	C	T	0.53977	Missense	p.T1111M	COSMIC
BCORL1	T46	chrX	129 147 806	C	T	0.47740	Missense	p.P353L	None
BRCA2	T39	chr13	32 906 921	A	G	0.40000	Missense	p.K436E	None
BRD4	T37	chr19	15 376 223	G	A	0.44444	Missense	p.A264V	None
BRIP1	T81	chr17	59 885 858	C	G	0.42308	Missense	p.E296D	None
CD58	T39	chr1	117 061 887	T	C	0.85185	Missense	p.I237V	None
CDH23	T34	chr10	73 501 454	G	A	0.40785	Missense	p.V1541M	None
CHD8	T46	chr14	21 894 360	G	T	0.46903	Missense	p.T269N	None
CHD8	T55	chr14	21 859 651	C	T	0.48592	Missense	p.E2067K	None
CIITA	T55	chr16	11 004 047	C	T	0.44654	Missense	p.T940M	None
CIITA	T56	chr16	11 000 940	G	A	0.43501	Missense	p.G531S	None
CMY45	T33	chr5	79 034 658	G	C	0.36957	Missense	p.S3357T	None
COL6A3	T39	chr2	238 296 329	G	A	0.42345	Missense	p.P403L	COSMIC
COL6A3	T55	chr2	238 277 596	G	A	0.38728	Missense	p.R1504W	COSMIC
CREBBP	T33	chr16	3 824 628	C	G	0.40741	Missense	p.R704P	None
CREBBP	T52	chr16	3 778 708	C	T	0.42241	Missense	p.G2076S	None
CUL9	T34	chr6	43 154 017	C	G	0.51064	Missense	p.Q359E	Ref. 15
DDX3X	T46	chrX	41 204 494	A	T	0.48918	Nonsense	p.R363*	None
DNMT3A	T09	chr2	25 463 248	G	A	0.30313	Missense	p.R749C	COSMIC
DNMT3A	T26	chr2	25 467 432	CAT	C	0.19303	Frameshift	p.M548fs	None
FBXW7	T39	chr4	153 332 910	C	CAGG	0.42920	Codon insertion	p.15_16insP	COSMIC
FBXW7	T81	chr4	153 268 155	TG	T	0.17647	Frameshift	p.Q100fs	COSMIC
FOXO1	99-31720	chr13	41 240 039	C	G	0.31250	Missense	p.G104A	None
FOXO1	T46	chr13	41 240 273	G	A	0.25547	Missense	p.P26L	None
FYB	T59	chr5	39 202 971	C	A	0.37037	Missense	p.G31V	None
IDH2	T06	chr15	90 645 600	A	G	0.41176	Missense	p.V8A	None
IL7R	T39	chr5	35 876 541	C	T	0.45918	Nonsense	p.Q445*	None
IRF4	T39	chr6	394 888	C	G	0.37700	Missense	p.T95R	None
IRF8	T39	chr16	85 936 739	T	A	0.38928	Missense	p.W40R	None
JAK3	T52	chr19	17 937 710	G	A	0.44845	Missense	p.L1073F	None
KDM4C	T46	chr9	7 046 915	T	A	0.30758	Missense	p.N771K	None
KDM6A	99-31720	chrX	44 941 837	G	GT	0.54369	Frameshift	p.R1054fs	None
KDM6A	T46	chrX	44 733 220	C	T	0.42655	Missense	p.A71V	None
KDM6A	T56	chrX	44 913 193	C	CT	0.41379	Frameshift	p.G291fs	None
KIAA1618	T52	chr17	78 264 463	AGAG	A	0.42010	Codon deletion	p.G404del	None
LRRK1	T34	chr15	101 514 110	C	T	0.36364	Missense	p.R67C	None
LRRK1	T34	chr15	101 549 251	C	G	0.34553	Missense	p.D324E	None
LRRK1	T59	chr15	101 567 909	G	A	0.41379	Missense	p.D865N	None
MLL	T33	chr11	118 366 578	C	T	0.32051	Missense	p.P1840S	None
MLL	T46	chr11	118 373 835	A	G	0.43956	Missense	p.M2407V	None
MLL2	99-31720	chr12	49 434 709	G	A	0.51190	Missense	p.R2282W	None
MLL2	T08	chr12	49 445 392	G	T	0.51471	Missense	p.P692T	Ref. 8
MLL2	T73	chr12	49 433 883	G	A	0.44056	Missense	p.P2557L	None
MLL2	T81	chr12	49 448 530	C	G	0.32143	Missense	p.G61R	None
MPDZ	T39	chr9	13 192 237	C	A	0.67901	Nonsense	p.E621*	None
NF1	T69	chr17	29 553 477	A	AC	0.30303	Frameshift	p.P678fs	COSMIC
PASD1	T34	chrX	150 844 560	C	T	0.39912	Missense	p.A756V	None
PASK	T06	chr2	242 080 117	C	T	0.41535	Missense	p.C83Y	None
PCLO	T04	chr7	82 763 889	T	A	0.31897	Missense	p.S993C	None
PCLO	T39	chr7	82 546 098	C	T	0.41736	Missense	p.G3735E	None
PCLO	T39	chr7	82 583 972	G	T	0.40136	Missense	p.D2099E	None
PCLO	T46	chr7	82 595 148	T	G	0.25290	Missense	p.E1319A	None
PHLPP	T04	chr18	60 645 819	G	A	0.47619	Missense	p.G925S	None
PLCG2	T55	chr16	81 902 872	G	A	0.48000	Missense	p.S178N	None
RELN	T37	chr7	103 136 199	T	C	0.48413	Missense	p.I3114V	None
SAMD9	T55	chr7	92 731 734	C	A	0.38095	Missense	p.R1226I	None
SETBP1	T38	chr18	42 456 670	C	CTCTT	0.19608	Frameshift	p.T228fs	None

Table 1. (Continued)

Gene	Case	CHR	POS	REF	ALT	Mutant Allele Fraction	Type	Effect	Previous Report
SETBP1	T56	chr18	42 456 691	A	C	0.25641	Missense	p.E234D	None
SMARCA2	T73	chr9	2 039 844	A	T	0.41176	Missense	p.Q245L	None
STAT5B	T81	chr17	40 375 521	C	G	0.38710	Missense	p.Q143H	None
TET1	T34	chr10	70 333 197	G	C	0.42177	Missense	p.A368P	None
TET1	T58	chr10	70 426 857	C	T	0.38255	Missense	p.T1506I	None
TET2	T31	chr4	106 193 809	CT	C	0.36364	Frameshift	p.S1424fs	COSMIC
TET2	T65	chr4	106 157 694	GCAATATTT		0.30000	Frameshift	p.Q866fs	COSMIC
TET2	T69	chr4	106 164 733	C	T	0.28571	Missense	p.R1201C	None
TNFAIP3	T02	chr6	138 195 991	A	G	0.39706	Missense	p.N102S	COSMIC
TNFAIP3	T37	chr6	138 201 240	A	C	0.48916	Missense	p.T647P	COSMIC
TNFAIP3	T73	chr6	138 201 240	A	C	0.37647	Missense	p.T647P	COSMIC
TNFRSF14	T61	chr1	2 488 104	A	G	0.16413	Missense; Start codon	p.M1V	COSMIC
TP53	T04	chr17	7 579 492	TCTGGGAGCTTCATCTGGAC		0.31169	Frameshift	p.G59fs	COSMIC
TP53	T56	chr17	7 578 190	T	C	0.86620	Missense	p.Y220C	COSMIC
TRAF3	T73	chr14	103 363 658	C	T	0.52830	Nonsense	p.Q294*	COSMIC
ULK4	T81	chr3	41 860 984	C	CT	0.21053	Frameshift	p.N594fs	None
ZAP70	T38	chr2	98 351 166	G	C	0.21287	Missense	p.R358P	None
ZAP70	T39	chr2	98 354 531	C	T	0.36923	Missense	p.P566L	None
ZFHX3	T34	chr16	72 831 834	C	A	0.37500	Missense	p.G1583C	None
ZMYM3	T38	chrX	70 469 934	G	C	0.33333	Missense	p.P398R	None
ZNF608	T46	chr5	123 985 372	A	G	0.39334	Missense	p.V394A	None

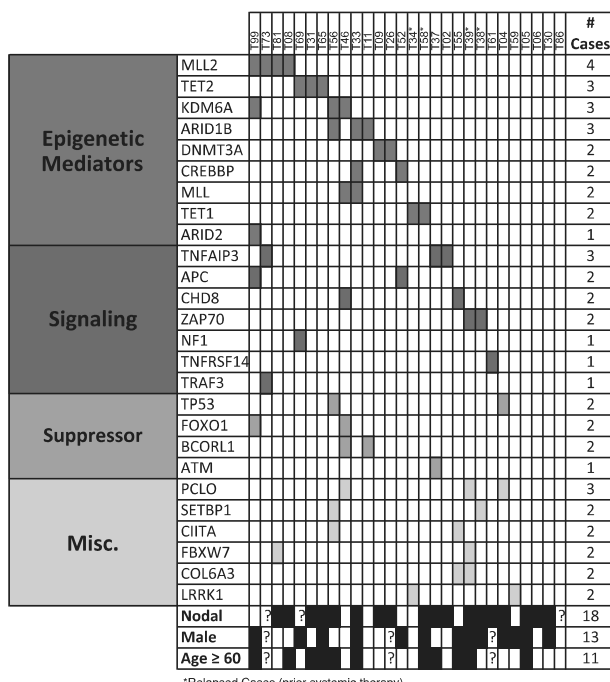


Figure 1. Distribution of mutations in 28 diagnostic peripheral T-cell lymphoma not otherwise specified (PTCL-NOS) cases. Included are all genes affected in multiple cases, or those affected in single cases with mutations listed in COSMIC or other reports as indicated in Table 1. Nodal: original presentation as nodal disease (black boxes) vs original extranodal presentation (white boxes).

Examination of survival effects (Supplementary Figure 2B) showed cases with alterations in histone methylation (*MLL2*, *KDM6A*, or *MLL*; $P=0.0198$) had worse OS than unaffected cases, whereas there was no such effect for either DNA methylation (*TET2*, *DNMT3A*, or *TET1*; $P=0.2694$) or signaling (*TNFAIP3*, *APC*, *CHD8*, *ZAP70*, *NF1*, *TNFRSF14*, or *TRAFF3*; $P=0.6695$). We also examined differences in mutational patterns between cases with

nodal or extranodal presentation (Supplementary Table 3). Although there was no significant difference in the above categories, interestingly all four cases affected by WNT/β-Catenin alterations were in the extranodal category ($P=0.003$).

Our study sheds new light on pathogenesis of a poorly understood clinical entity in need of better therapeutic options and for which poor sample availability has limited interrogation of the mutational landscape to date. Although some findings are confirmatory, others highlight novel disease mechanisms or better define frequency or prognostic implications. In particular, histone methylation alterations were present in a quarter of cases and associated with a worse OS. We believe studies in additional case series are warranted for elaboration of this result. Frequent mutations in regulators of TCR signaling meanwhile highlight mechanisms of activation, further extending the importance of this pathway beyond cases containing the previously identified ITK-SYK fusion kinase. The clustering of all mutations affecting WNT/β-Catenin mediators *APC* or *CHD8* in cases with an extranodal presentation represented a significant difference that should be explored in additional cases and could shed new light on extranodal PTCL-NOS. Therapeutic opportunities from some results are limited. Loss of function of *A20*, for example, does not easily lend itself to targeted treatment, as NF-κB Inducing Kinase inhibitors have not made their way to clinical evaluation. Low frequency of *TP53* mutations, however, highlights a potential for MDM2 inhibition in PTCL-NOS. In sum, we identify promising candidates for evaluation in additional cases and functional studies and to aid the development of better model systems for one of the least well understood hematologic malignancies.

CONFLICT OF INTEREST

The authors declare no conflict of interest.

ACKNOWLEDGEMENTS

This research was supported by Cycle for Survival (JS and all MSKCC authors), the Gabrielle's Angel Foundation (JS), the Lymphoma Research Foundation (JS), NCI R01-CA142798-01 (HGW), the Leukemia Research Foundation (HGW), the Experimental Therapeutics Center at MSKCC (HGW), the American Cancer Society 10284 (HGW), the

Geoffrey Beene Cancer Center (HGW), an American Cancer Society Research Scholar Grant (DW) and Nonna's Garden Fund (SH).

AUTHOR CONTRIBUTIONS

JS designed the research and wrote the manuscript. HGW, SH and DW designed the research and edited the manuscript. ML, AV, AH and KH designed the research. JT-F designed the research and reviewed the pathology of included cases. NL, ID, NS and MP performed bioinformatic analyses. JM collected and helped analyze clinical data.¹⁵

JH Schatz^{1,2,3}, SM Horwitz⁴, J Teruya-Feldstein⁵, MA Lunning⁴, A Viale⁶, K Huberman⁶, ND Socci⁷, N Lailler⁶, A Heguy⁸, I Dolgalev⁸, JC Migliacci⁴, M Pirun⁷, ML Palomba⁴, DM Weinstock⁹ and H-G Wendel¹⁰

¹Department of Medicine, Tucson, AZ, USA;

²Bio5 Institut, Tucson, AZ, USA;

³Department of Pharmacology & Toxicology University of Arizona, Tucson, AZ, USA;

⁴Department of Medicine, New York, NY, USA;

⁵Department of Pathology, New York, NY, USA;

⁶Genomic Core Laboratory, New York, NY, USA;

⁷Bioinformatics Core, New York, NY, USA;

⁸Genome Technology Center, New York University Langone Medical Center, New York, NY, USA;

⁹Department of Medical Oncology, Dana-Farber Cancer Institute, Boston, MA, USA and

¹⁰Cancer Biology & Genetics Program Memorial Sloan-Kettering Cancer Center, New York, NY, USA

E-mail: schatzj@email.arizona.edu or horwitzs@mskcc.org

REFERENCES

- Iqbal J, Wright G, Wang C, Rosenwald A, Gascoyne RD, Weisenburger DD et al. Gene expression signatures delineate biologic and prognostic subgroups in peripheral T-cell lymphoma. *Blood* 2014; **123**: 2915–2923.
- Vose J, Armitage J, Weisenburger D. International T-Cell Lymphoma Project. International peripheral T-cell and natural killer/T-cell lymphoma study: pathology findings and clinical outcomes. *J Clin Oncol* 2008; **26**: 4124–4130.
- Cairns RA, Iqbal J, Lemonnier F, Kucuk C, de Leval L, Jais JP et al. IDH2 mutations are frequent in angioimmunoblastic T-cell lymphoma. *Blood* 2012; **119**: 1901–1903.

Supplementary Information accompanies this paper on the Leukemia website (<http://www.nature.com/leu>)

The importance of central pathology review in international trials: a comparison of local versus central bone marrow reticulin grading

Leukemia (2015) **29**, 241–244; doi:10.1038/leu.2014.262

Central pathology review for multicenter clinical trials was first introduced in the 1960s as an important quality control measure for lymphoma diagnoses.¹ Although widely recognized as an essential measurement of quality assurance and in use for over half a century, only rare reports exist comparing the histopathological evaluation of hematopoietic neoplasms between the central review and the contributing local pathologists in clinical

Letters to the Editor

241

- Palomero T, Couronné L, Khiabanian H, Kim M-Y, Ambesi-Impiombato A, Perez-Garcia A et al. Recurrent mutations in epigenetic regulators, RHOA and FYN kinase in peripheral T cell lymphomas. *Nat Genet* 2014; **46**: 166–170.
- Sakata-Yanagimoto M, Enami T, Yoshida K, Shiraishi Y, Ishii R, Miyake Y et al. Somatic RHOA mutation in angioimmunoblastic T cell lymphoma. *Nat Genet* 2014; **46**: 171–175.
- Lemonnier F, Couronne L, Parrens M, Jais JP, Travert M, Lamant L et al. Recurrent TET2 mutations in peripheral T-cell lymphomas correlate with TFH-like features and adverse clinical parameters. *Blood* 2012; **120**: 1466–1469.
- Odejide O, Weigert O, Lane AA, Toscano D, Lunning MA, Kopp N et al. A targeted mutational landscape of angioimmunoblastic T cell lymphoma. *Blood* 2013; **123**: 1293–1296.
- Rossi D, Pasqualucci L, Trifonov V, Fangazio M, Bruscaggin A, Rasi S et al. The coding genome of splenic marginal zone lymphoma: activation of NOTCH2 and other pathways regulating marginal zone development. *J Exp Med* 2012; **209**: 1537–1551.
- Kadoch C, Hargreaves DC, Hodges C, Elias L, Ho L, Ranish J et al. Proteomic and bioinformatic analysis of mammalian SWI/SNF complexes identifies extensive roles in human malignancy. *Nat Genet* 2013; **45**: 592–601.
- Streubel B, Vinatzer U, Willheim M, Raderer M, Chott A. Novel t(5;9)(q33;q22) fuses ITK to SYK in unspecified peripheral T-cell lymphoma. *Leukemia* 2005; **20**: 313–318.
- Pechloff K, Holch J, Ferch U, Schwenecker M, Brunner K, Kremer M et al. The fusion kinase ITK-SYK mimics a T cell receptor signal and drives oncogenesis in conditional mouse models of peripheral T cell lymphoma. *J Exp Med* 2010; **207**: 1031–1044.
- Lee EG, Boone DL, Chai S, Libby SL, Chien M. Failure to regulate TNF-induced NF-κB and cell death responses in A20-deficient mice. *Science* 2000; **289**: 2350–2354.
- Matsushima AY, Cesarman E, Chadburn A, Knowles DM. Post-thymic T cell lymphomas frequently overexpress p53 protein but infrequently exhibit p53 gene mutations. *Am J Pathol* 1994; **144**: 573–584.
- Petit B, Leroy K, Kanavaros P, Boulland ML, Druet-Cabanac M, Haioun C et al. Expression of p53 protein in T- and natural killer-cell lymphomas is associated with some clinicopathologic entities but rarely related to p53 mutations. *Hum Pathol* 2001; **32**: 196–204.
- Chang H, Jackson DG, Kayne PS, Ross-Macdonald PB, Ryseck R-P, Siemers NO. Exome sequencing reveals comprehensive genomic alterations across eight cancer cell lines. *PLoS One* 2011; **6**: e21097.



This work is licensed under a Creative Commons Attribution-NonCommercial-NoDerivs 4.0 International License. The images or other third party material in this article are included in the article's Creative Commons license, unless indicated otherwise in the credit line; if the material is not included under the Creative Commons license, users will need to obtain permission from the license holder to reproduce the material. To view a copy of this license, visit <http://creativecommons.org/licenses/by-nc-nd/4.0/>

Accepted article preview online 3 September 2014; advance online publication, 3 October 2014